

ISTITUTO NAZIONALE DI FISICA NUCLEARE

Sezione di Trieste

INFN/AE-92/30

30 novembre 1992

G. Cantatore, F. Della Valle, E. Milotti and C. Rizzo

**A MEASUREMENT OF THE VACUUM
BIREFRINGENCE INDUCED BY A MAGNETIC
FIELD WITH HIGH ENERGY PHOTONS**

A Measurement of the Vacuum Birefringence Induced by a Magnetic Field with High Energy Photons

G.Cantatore, F. Della Valle, E.Milotti

Dipartimento di Fisica dell'Università di Trieste and INFN-Sezione di Trieste,
Via Valerio 2, I-34127 Trieste, Italy

and

C.Rizzo

INFN-Sezione di Trieste, Padriciano 99, I-34012 Trieste, Italy

Presented by E.Milotti

at the Workshop on "European Electron Facility", Mainz, Oct. 7-9 1992

Abstract

In QED photons interact - very weakly - with a magnetic field. This paper summarizes the physics motivations for trying to detect this minute effect, and presents a set-up to measure it with high energy photons obtained by Compton backscattering an intense visible laser beam off an electron beam. Such a set-up might eventually be used in a machine like the proposed EEF.

1. Introduction and theoretical overview.

The linearity of the Maxwell equations of classical electrodynamics implies that in vacuum there is no light-light interaction, and similarly there is no interaction between light and field (be it electric or magnetic). However it was shown long ago by Euler and Heisenberg [1] and by Weisskopf [2], that the electromagnetic field lagrangian is modified by the vacuum fluctuations of the electronic field (and other matter fields) so that these interactions may actually take place. It is also quite noteworthy that this is one of the very few non perturbative results of quantum electrodynamics as it uses the exact solution of the Dirac equation in an external almost constant electromagnetic field. In the modern language of Feynman diagrams this means that the Euler-Heisenberg-Weisskopf (EHW) result for the propagation of a photon in an external almost constant field takes into account all the diagrams shown in figure 1. The “classical” nature of the external field appears from the absence of diagrams with internal virtual photon lines.

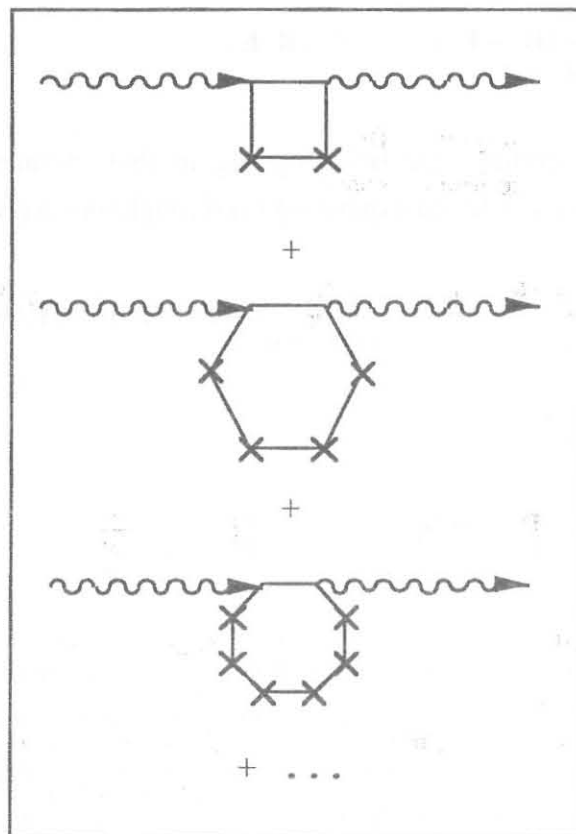


Figure 1: The diagrammatic perturbative expansion equivalent to the EHW result (the crosses denote interactions with the external field and the permutations of the vertices are implicitly assumed).

Notice that according to Furry's theorem the only non vanishing diagrams have an even number of photon lines attached to the electron loop, thus the lowest order interaction has four vertices on the loop and this helps to account for the smallness of the effect. Besides this there are other kinematical restrictions (see [3,4] for a complete account of the underlying theory).

The EHW effective lagrangian (in the form rederived later by Schwinger [5]) is

$$\mathcal{L} = -\frac{\mathcal{F}}{4\pi} - \frac{1}{8\pi^2} \int_0^\infty \frac{ds}{s^3} \exp(-m^2 s) \left\{ (es)^2 L - 1 - \frac{2}{3} (es)^2 \mathcal{F} \right\} \quad (1)$$

where the usual convention $\hbar = c = 1$ has been used and

$$L = i\mathcal{G} \frac{\cosh\{es[2(\mathcal{F} + i\mathcal{G})]^{1/2}\} + \cosh\{es[2(\mathcal{F} - i\mathcal{G})]^{1/2}\}}{\cosh\{es[2(\mathcal{F} + i\mathcal{G})]^{1/2}\} - \cosh\{es[2(\mathcal{F} - i\mathcal{G})]^{1/2}\}};$$

$$\mathcal{F} = \frac{1}{2}(\mathbf{B}^2 - \mathbf{E}^2); \quad \mathcal{G} = \mathbf{B} \cdot \mathbf{E}.$$

Then the electromagnetic field lagrangian that includes the lowest order diagram in figure 1 can be found expanding (1) through fourth order

$$\mathcal{L} = \frac{1}{8\pi}(\mathbf{E}^2 - \mathbf{B}^2) + \frac{2\alpha^2}{45(4\pi)^2 m^4} [(\mathbf{E}^2 - \mathbf{B}^2) + 7(\mathbf{E} \cdot \mathbf{B})], \quad (2)$$

and the fields \mathbf{D} and \mathbf{H} are

$$\mathbf{D} = 4\pi \frac{\partial \mathcal{L}}{\partial \mathbf{E}} \quad \text{and} \quad \mathbf{H} = -4\pi \frac{\partial \mathcal{L}}{\partial \mathbf{B}}. \quad (3)$$

This lowest order diagram appears in physical processes other than light-field scattering, e.g. as a radiative correction to the g-2 diagrams and as a correction to Compton scattering off nuclei (and in that case it is known as Delbrück scattering). However in the case of the correction to g-2 all the photon lines are virtual. In addition to this the g-2 vertex must be renormalized to prevent a logarithmic divergence even at its lowest perturbative order [6].

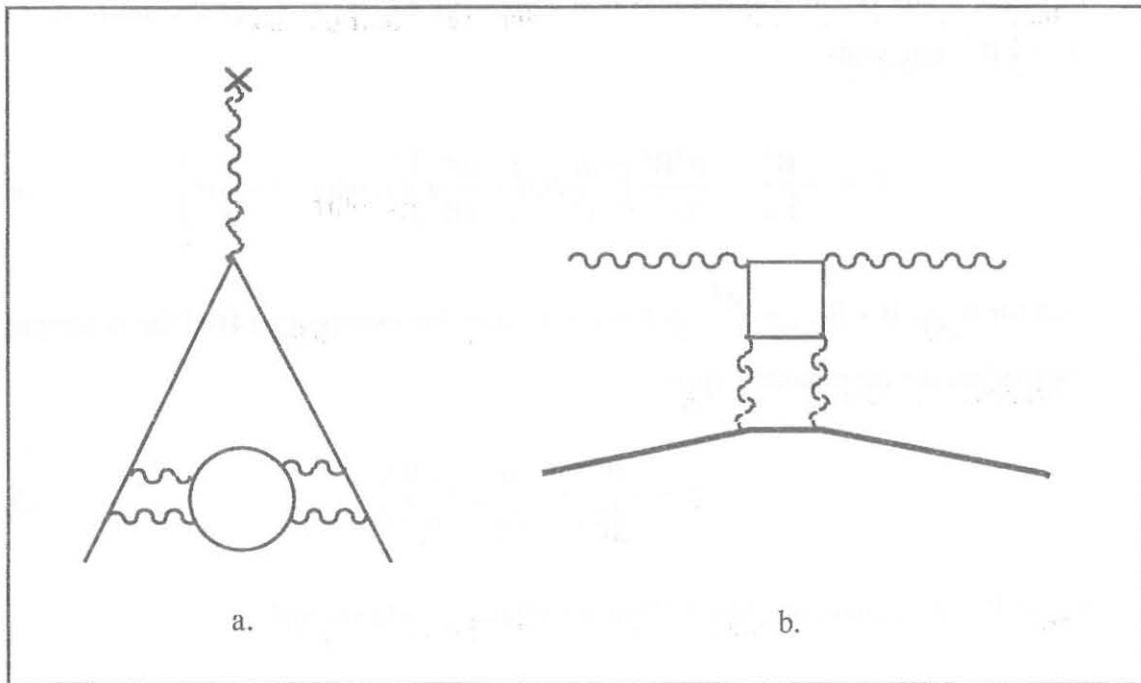


Figure 2: The lowest order diagram as a radiative correction to $g-2$ (a.) and as Delbrück scattering of light off nuclei (b.).

On the other hand Delbrück scattering seems to be a genuine light-field scattering in the same sense implied by figure 1, and indeed it is, but the point is that it cannot be described by the lagrangian (1). Remember that (1) was derived with the assumption of almost constant field, and this is not the case for the electric field of a nucleus. Moreover experimentally it appears as a radiative correction to Compton scattering. These facts make both the calculation of Delbrück scattering and its observation very difficult [7].

To summarize, the point that we wish to make is that the observation of light-field scattering amounts to a direct observation of vacuum polarization, without the theoretical or practical difficulties that are present in other processes.

In the past other authors that have presented similar experiments have argued that the observation of light-field scattering “is well worth the effort on aesthetic, if no other, grounds” [8]. On the contrary, we want to stress here that the non linearity of the EHW lagrangian opens the door to very interesting and fundamental speculations: consider for instance the following argument. It is well known that on sheer dimensional grounds it can be conjectured that there is a “critical” magnetic (and electric) field strength $|\mathbf{B}_{cr}| \approx \frac{m^2 c^3}{e \hbar} \approx 4.4 \cdot 10^{13} \text{ gauss}$, so that *something* should happen at high field strengths, and indeed using the lagrangian (1) one finds that the

effective fields \mathbf{D} and \mathbf{H} reach maximal values [9]. So, if one takes the limit $\mathcal{G} \rightarrow 0$, $\mathcal{F} \rightarrow \frac{1}{2} \mathbf{B}^2$, one finds

$$\mathcal{L} = -\frac{\mathbf{B}^2}{8\pi} - \frac{\alpha^2 \mathbf{B}^2}{8\pi^2} \int_0^\infty \frac{dt}{t^3} \exp\left(-\frac{m^2}{eB} t\right) \left\{ t \coth t - 1 - \frac{1}{3} t^2 \right\} \quad (4)$$

then for fields $B \gg B_{\text{cr}} (= \frac{m^2}{e}$ in $\hbar = c = 1$ units) the expression (4) of the lagrangian approaches the asymptotic value:

$$\mathcal{L} \sim -\frac{\mathbf{B}^2}{8\pi} \left(1 - \frac{\alpha}{3\pi} \log \frac{\kappa B}{m^2} \right) \quad (5)$$

where κ is a constant of order 1. Thus the effective field strength is:

$$\mathbf{H} = -4\pi \frac{\partial \mathcal{L}}{\partial \mathbf{B}} \sim \mathbf{B} \left(1 - \frac{\alpha}{6\pi} - \frac{\alpha}{3\pi} \log \frac{\kappa B}{m^2} \right). \quad (6)$$

The same can be done for the electric field, taking the limit $\mathcal{G} \rightarrow 0$, and $\mathcal{F} \rightarrow -\frac{1}{2} \mathbf{E}^2$, so that for fields much larger than the critical field

$$\mathbf{D} = 4\pi \frac{\partial \mathcal{L}}{\partial \mathbf{E}} \sim \mathbf{E} \left(1 - \frac{\alpha}{6\pi} - \frac{\alpha}{3\pi} \log \frac{\kappa \mathbf{E}}{m^2} \right). \quad (7)$$

The new, striking feature introduced by the non linearity of the lagrangian is that now the effective field strength \mathbf{D} (or \mathbf{H}) does not grow indefinitely, but attains a maximum value when \mathbf{E} (or \mathbf{B}) is equal to $\frac{m^2}{\kappa} \exp\left(\frac{3\pi}{\alpha} - \frac{3}{2}\right)$. But $\mathbf{D} = \frac{e}{r^2}$, therefore if \mathbf{D} has a maximum then r has a minimum.

So one could only approach a charge up to a minimum distance, which might be taken as a charge radius for the electron, and quantum electrodynamics would self-heal its ultraviolet divergences by introducing a natural "minimal length". This electron radius is actually so small as to be inaccessible to direct observation: taking $\kappa = 1$ one finds $r_{\text{min}} \approx \lambda_e \cdot 10^{-281}$.

The arguments given above are not "proofs" (especially because it is hard to see how the lagrangian (1) could still hold for lengths shorter than the electron Compton wavelength), but just hints that it is quite important to test experimentally the non linearity of the lagrangian (1). For a full discussion of these conjectures we refer the

reader to [9], and we turn now to the problem of the experimental detection of light-field scattering.

2. Short review of previous and planned experiments.

Previous attempts to detect light-field scattering have always used intense visible laser beams and large magnetic fields (up to a few Tesla). From equations (2) and (3) it is fairly easy to see that the refractive index of vacuum changes when the magnetic field is present, and that it depends on the mutual orientation of light polarization and magnetic field, so that (with CGS system definitions [4])

$$n_{\parallel} = 1 + \frac{4e^4 \hbar}{90m^4 c^7} B^2 \sin^2 \theta \quad (8)$$

$$n_{\perp} = 1 + \frac{7e^4 \hbar}{90m^4 c^7} B^2 \sin^2 \theta$$

(here θ is the angle between the laser beam direction and the magnetic field). The arrangement of the region where the laser beam and the magnetic field interact is shown in figure 3. There $\theta = 0$, so that after one passage in the interaction region the phase shift between the \parallel and the \perp components is

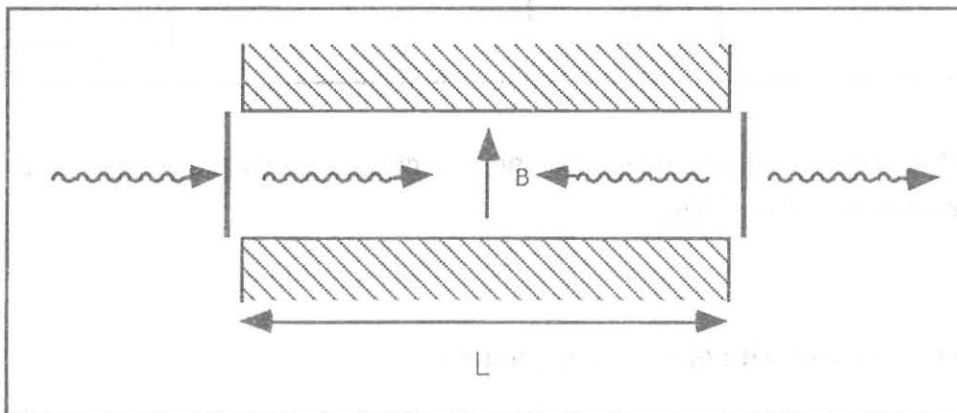


Figure 3: Typical layout of the interaction region for an experiment with visible photons. The polarized laser beam enters a Fabry-Perot cavity (or a multipass cavity) from the left. The thick lines represent the cavity mirrors, while the hatched regions are the polar expansions of the large magnet that provides the high magnetic field B . Photons bounce back and forth in the cavity before leaving from the mirror on the right.

$$\Delta\phi = \frac{2\pi L}{\lambda}(n_{\perp} - n_{\parallel}) = \frac{2\pi L}{\lambda} \left(\frac{e^4 \hbar}{30m^4 c^7} B^2 \right) \approx \frac{2\pi L}{\lambda} (1.2 \cdot 10^{-31}) B^2. \quad (9)$$

Even with large magnets ($L \sim 10$ m) and high fields ($B \sim 10$ T) the phase shift $\Delta\phi$ is quite small for visible lasers ($\lambda \sim 500$ nm), so that for one pass inside the cavity $\Delta\phi \sim 10^{-13}$ radians. Even with an optical cavity which “folds” the light beam and yields many passes inside the optical cavity, the total phase shift cannot be made larger than about 10^9 radians. This phase shift is much smaller than the random phase shifts introduced by environmental and instrumental noise, and one must resort to sophisticated optical and signal analysis techniques to detect it [10]. The last attempt to detect it fell short of its goal, while another ongoing attempt is expected to reach the required signal-to-noise ratio [11]. The overall experimental layout is shown in figure 4 [10].

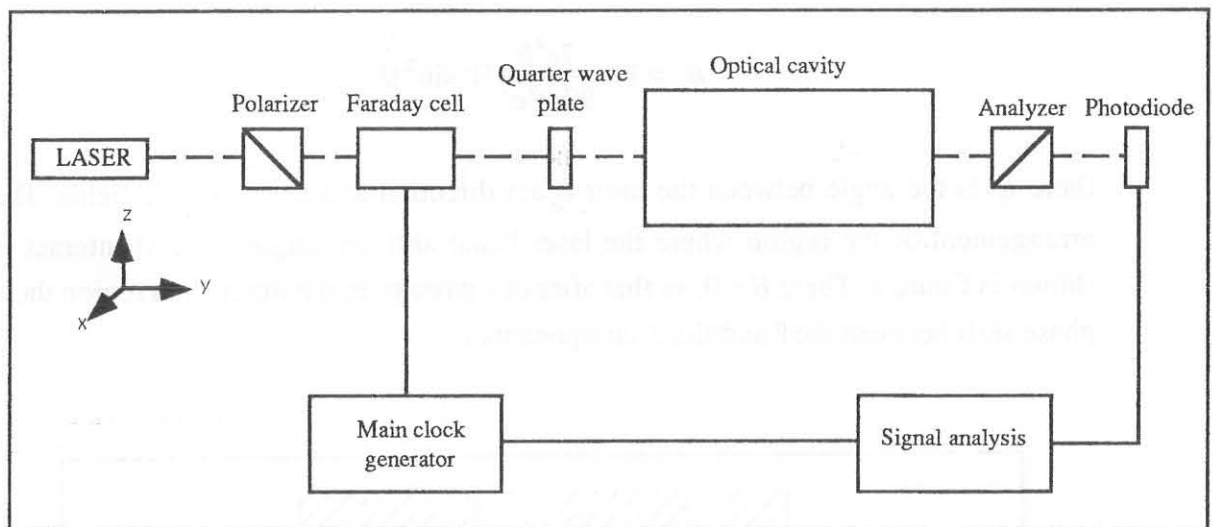


Figure 4: Typical experimental apparatus (simplified) for the experiment with visible photons (adapted from [10]).

3. An experiment with high energy photons.

Equations (8) are approximate, but they hold over a very wide photon energy range [4], as the photon energy must be $\hbar\omega(eV) \ll \frac{2 \cdot 10^{19}}{B(\text{gauss})}$. Since the phase shift (9) is inversely proportional to the photon wavelength, it can be made larger using higher energy photons, so that one might achieve a measurable effect with just one pass in the magnetic field region, and avoid several systematic errors and much of the

environmental and experimental noise that appears in the experiments described in section 2.

As a source of high energy polarized photons we propose to use the Compton backscattering of a polarized laser beam on a high energy electron beam. At high photon energy one may use oriented crystals as polarization analyzers [12,13]. In these crystals the absorption rates for the high energy photons depend on the orientation of the polarization axis with respect to the crystal symmetry axes due to the interference effects observed in the high energy production of the electron pairs.

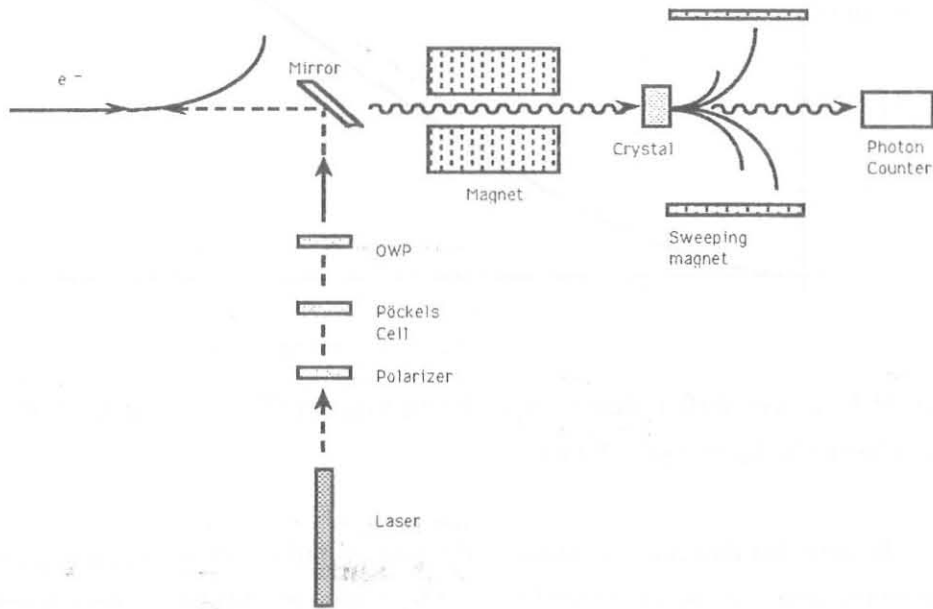


Figure 5: Layout of the experiment with high energy photons.

The layout of the apparatus is shown in figure 5: a continuous-wave laser beam is linearly polarized and then crosses a quarter-wave plate so that it becomes circularly polarized; it is deflected by a thin mirror into a straight section of the electron machine. The optical photons are backscattered into high energy photons by the electrons: if the electron energy is not very high ($< 40\text{-}50\text{ GeV}$), the electrons act as “mirrors”, and preserve the initial photon polarization [14]. The high energy electrons are bent away by the dipole magnets in the machine, while the high energy circularly polarized photons pass through a high magnetic field region, which acts as a birefringent medium, and are eventually analyzed by an oriented crystal - which is the final polarizer - and by a photon counter. The polarizing action of the oriented crystal is due to different pair-production cross-sections for different polarization states: therefore the pair-produced electrons must be swept away by a small magnet. The phase shift after the traversal of the magnetic field is small (see figure 6), but still

a few orders of magnitude above the corresponding phase shift acquired by visible photons as in [10,11].

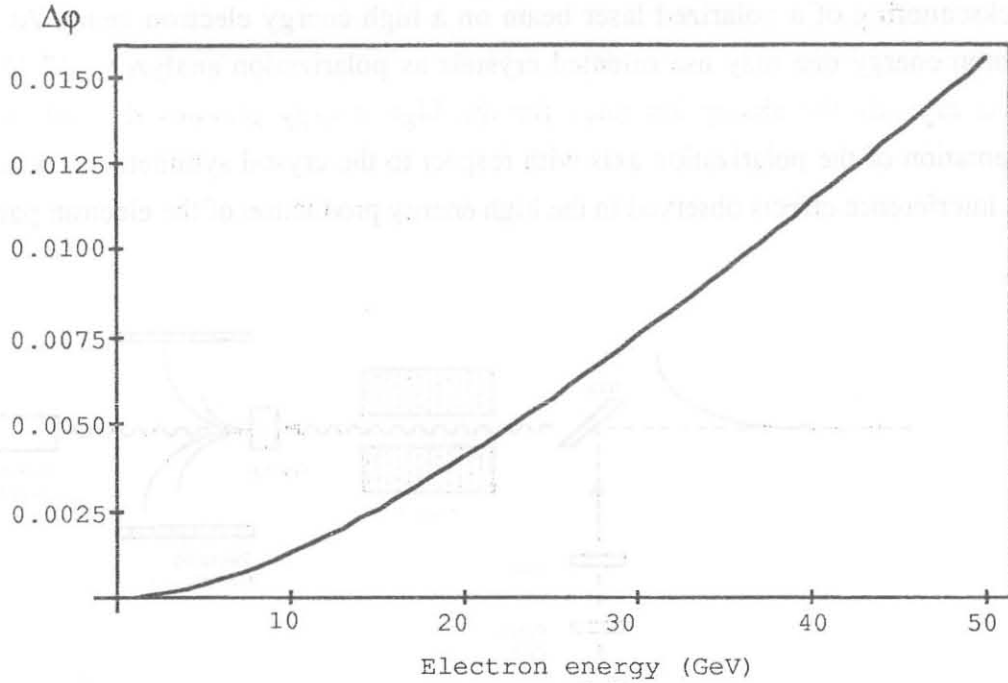


Figure 6: Phase shift induced by a strong magnet ($B_0 = 10$ Tesla, $L = 10$ m), for a green laser (Ar laser, $\hbar\omega \approx 2.5$ eV)

It turns out that the evolution of the photon polarization, including the Compton scattering step, can be completely described with the Müller matrix formalism (see [15] for a description of the formalism applied to Compton scattering, and [16] for the details of the calculation).

The result of the detailed calculation is that the total cross-section for the detection of high energy half of the photon spectrum in the electromagnetic calorimeter after the analyzer (which has its axis at a 45° angle with respect to \mathbf{B}) is

$$\sigma \approx \frac{3}{16} \sigma_T T A (1+\epsilon^2) \left[1 \pm \Delta\phi \frac{D(1-\epsilon^2)}{A(1+\epsilon^2)} \right] \quad (10)$$

where σ_T is the classical Thomson cross-section $\sigma_T = \frac{8\pi}{3} r_0^2$, T is the transmittivity of the polarizer and ϵ^2 is its extinction coefficient, and A and D are given by (8) and (9) in [16], and are shown in figure 7 as functions of the electron energy. The \pm sign refers to left and right circular polarizations, so that one can detect an asymmetry in the photon count after switching the photon polarization state.

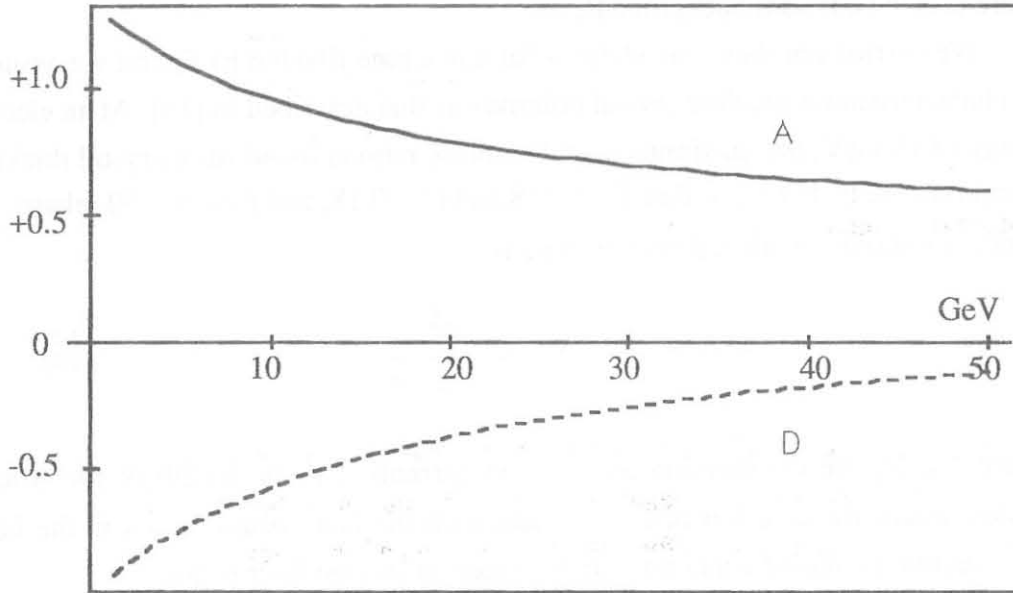


Figure 7: The coefficients A and D vs. the electron energy.

The number of detected photons per unit time is proportional to $T A (1+\epsilon^2)$, while in order to have a signal-to-noise ratio = 1 one needs

$$N_{\text{TOT}} \sim \left\{ \Delta\phi \frac{D (1-\epsilon^2)}{A (1+\epsilon^2)} \right\}^{-2} \quad (11)$$

photons, therefore the total measurement time is inversely proportional to

$$T A (1+\epsilon^2) \left\{ \Delta\phi \frac{D (1-\epsilon^2)}{A (1+\epsilon^2)} \right\}^2. \quad (12)$$

Since T and ϵ^2 are functions of the crystal thickness, one can optimize the crystal so that it has the highest analyzing power and the highest transmittivity.

The machine background can also be easily accounted for; it cannot depend on the field \mathbf{B} , and therefore it modifies only the A constant in (10): it amounts to a constant “noise”, and just raises the number of photon counts needed to carry out a measurement. Thus (10) is changed to

$$\sigma \approx \frac{3}{16} \sigma_T T \left[A (1+\epsilon^2) \pm D (1-\epsilon^2) \Delta\phi \right] + C \quad (13)$$

where C is the constant background¹.

We carried out these calculations for a machine like the EEF, and we assumed the characteristics a graphite crystal polarizer as that described in [13]. At an electron energy of 15 GeV, the maximum signal-to-noise ratio is found for a crystal thickness of approximately 48 cm, so that $T \approx 0.148$ and $\epsilon^2 \approx 0.18$, and then $\sigma \approx 30$ mbarn. The number of photons analyzed per unit time is

$$N_e \cdot N_\gamma \cdot \frac{2l}{c} \cdot \frac{\sigma}{s} \quad (14)$$

where N_e , N_γ are the electron and photon currents, l is the length of the straight section where the electron beam interacts with the laser beam, and s is the beam cross-section (assumed equal for both the electron and the laser beam).

Then, if

$$B \approx 10 \text{ T}$$

$$L \approx 10 \text{ m}$$

$$N_e \approx 3 \cdot 10^{14} \text{ electrons/s} \quad (\approx 50 \mu\text{A})$$

$$N_\gamma \approx 1.3 \cdot 10^{19} \text{ photons/s} \quad (\text{this corresponds to a 5W CW Ar laser, for which } h\omega \approx 2.5 \text{ eV})$$

$$l \approx 1000 \text{ m}$$

$$s \approx 3 \cdot 10^{-6} \text{ m}^2$$

it takes $\sim 1.7 \cdot 10^7$ high energy photons to reach a signal-to-background ratio ≈ 1 , and (14) gives 25000 analyzed photons/s. Thus it takes $\sim 6.8 \cdot 10^2$ seconds to see the effect, and including another factor 2 to account for background, this would give $\sim 1.4 \cdot 10^3$ seconds.

4. Conclusions.

Taking the advertised machine parameters it is possible to detect light-field scattering at the EEF, using a set-up like the one described here. We wish to remark that the thick graphite crystal that has been proposed as analyzer of polarization at high energy might be substituted by a thin crystal where the pair-produced electrons - rather than the photons that have not been absorbed - are observed. Such a scheme has already been proposed to observe the longitudinal electron polarization in machines

¹ We cannot estimate the background in the EEF at the moment of writing, but the background for other machines such as LEP can be easily estimated from measurements like those in [17]

such as LEP [18]. Actually, the apparatus that we propose, is almost the same as the longitudinal polarization monitors that have been planned for LEP and other machines. The only difference is that we should have a high field magnet in the photon path. Thus one might carry out this experiment in “parasitic” mode along with polarization monitoring. Figure 8 shows how a polarization monitor might fit into a CEBAF-like EEF, out of the way of the experimental areas.

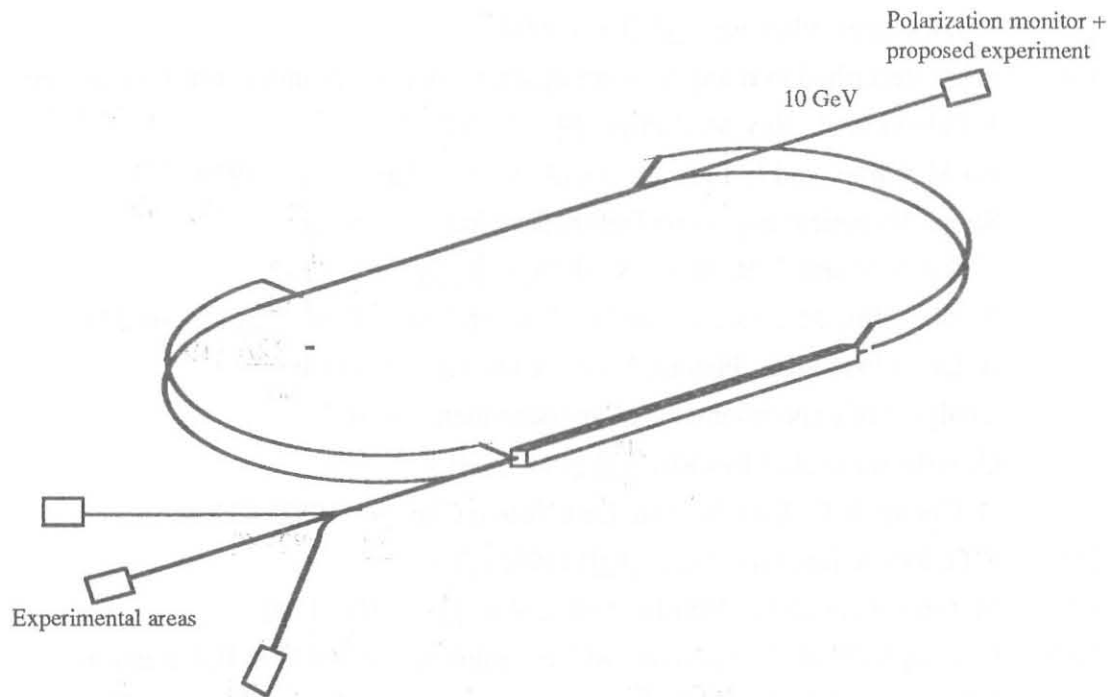


Figure 8: General layout.

Given the short time it would take to achieve a signal-to-noise ratio of 1, and taken for granted the parasitic mode, this set-up would contribute a high accuracy test of lagrangian (1).

Acknowledgements.

We wish to acknowledge many useful discussions with Prof. E.Zavattini, who is the originator of this experimental line, and with Dr. R.Ragazzon.

References.

- [1] W. Heisenberg and H. Euler, *Z.Phys.* 98 (1936) 718
- [2] V. S. Weisskopf, *K.Dan.Vidensk.Selsk.Mat.Fys.Medd.*14 (1936) no. 6.
- [3] S. L. Adler, *Ann.Phys.* 67 (1971) 599
- [4] V. B. Berestetskii, E. M. Lifshitz and L. P. Pitaevskii, "Quantum Electrodynamics", Pergamon Press (Oxford 1976)
- [5] J. Schwinger, *Phys.Rev.* 82 (1951) 664
- [6] $g-2$ is described in many texts on quantum electrodynamics. For reviews see J. Calmet et al., *Rev.Mod.Phys.* 49 (1977) 21
F.J.M. Farley and E. Picasso, *Ann.Rev.Nucl.Part.Sci.* 29 (1979) 243,
- [7] Some theoretical papers on Delbrück scattering are e.g.
T. Bar-Noy and S. Kahane, *Nucl.Phys.* A288 (1977) 132,
B. De Tollis, M. Lusignoli and G. Pistoni, *Nuovo Cim.* 32A (1976) 227,
B. De Tollis and G. Pistoni, *Nuovo Cim.* 42A (1977) 499.
Analyses of experimental data are described, e.g. in
G. Jarlskog et al., *Phys.Rev.* D8 (1973) 3813,
H. Cheng, E-C. Tsai, X. Zhu, *Lett.Nuovo Cim.* 34 (1982) 427.
- [8] K.O. Mikaelian, *Phys.Lett.* 115B (1982) 267
- [9] M. Greenman and F. Rohrlich, *Phys.Rev.* D8 (1973) 1103
- [10] E. Iacopini et al.: "Experimental Determination of Vacuum Polarization Effects on a LASER Light-beam Propagating in a Strong Magnetic Field", CERN Proposal D2, 9 June 1980,
E. Iacopini and E. Zavattini, *Phys.Lett.* 85B (1979) 151,
E. Iacopini, B.Smith, G.Stefanini and E. Zavattini, *Nuovo Cim.* 61B (1981) 21
- [11] INFN Proposal PVLAS (1991)
- [12] G. Diambri Palazzi, *Rev.Mod.Phys.* 40 (1968) 611
- [13] R.L. Eisele et al., *Nucl.Instr.Meth.* 113 (1973) 489
- [14] R.H. Milburn, *Phys.Rev.Lett.* 10 (1963) 75
- [15] W.H. McMaster, *Rev.Mod.Phys.* 33 (1961) 8, and also W.H. McMaster, *Am.J.Phys.* 22 (1954) 351
- [16] G. Cantatore, F.Della Valle, E. Milotti, L. Dabrowski and C. Rizzo, *Phys.Lett.* B265 (1991) 418
- [17] B. Dehning et al., *Phys.Lett.* B249 (1990) 145
- [18] M. Placidi and R. Rossmanith, *Nucl.Instr.Meth.* A274 (1989) 79